Chemical, structural, and transport properties of $Na_{1-x}CoO_2$

F. Rivadulla, J.-S. Zhou, and J. B. Goodenough
Texas Materials Institute, ETC 9.102, The University of Texas at Austin, 1 University Station, C2201, Austin, Texas 78712, USA
(Received 4 April 2003; revised manuscript received 4 June 2003; published 14 August 2003)

We report measurements of room-temperature compressibility, thermal expansion, thermoelectric power α(T) at various pressures $P \leqslant 20$ kbar, basal-plane resistivity $\rho_{ab}(T)$, magnetic susceptibility, and thermal conductivity $\kappa(T)$ taken on single-crystal or cold-pressed $Na_{1-x}CoO_2$, $(1-x) \approx 0.57$. Whereas the *c*-axis thermal expansion is large, the basal-plane thermal expansion remains negligible for all temperatures $T < 300$ K. We propose here that pinning of the nominal Co(IV)/Co(III) redox couple at the top of the $O^{2-}:2p^6$ bands, and a schematic location of the a_1^T and e^T antibonding bands of this couple with respect to the Fermi energy are responsible for the large thermoelectric power found in this compound. On the other hand, the phonon contribution to the thermal conductivity measured on a dense cold-pressed ceramic sample is not as small as previously reported.

DOI: 10.1103/PhysRevB.68.075108 PACS number(s): 72.15.−v, 65.40.−b, 74.10.+v

I. INTRODUCTION

The layered oxides $A_{1-x}CoO_2$ all contain close-packed planes of low-spin, octahedral-site Co atoms sharing common octahedral-site edges; the *A* atoms occupy octahedral or trigonal-prismatic sites between the layers.[1] The Li^+ ions of $Li_{1-x}CoO_2$ remain in octahedral sites for all values of *x*, and the system has been extensively studied and commercialized since the demonstration[2] that it can be used as the cathode of a Li^+-ion rechargeable battery. As Li is extracted at room temperature, a flat open-circuit voltage of a $Li_{1-x}CoO_2$ cell in the range $0.05 < x < 0.25$ (Ref. 3) signals a first-order change from polaronic to itinerant in-plane conduction as *x* increases,[4] and oxygen evolution from the CoO_2 layers sets in for $x > 0.5$.[5] The Na^+ ions of the system $Na_{1-x}CoO_2$ change from octahedral to trigonal-prismatic coordination across a two-phase region as *x* increases in the range $0.15 < x < 0.22$,[6] but the CoO_2 sheets remain intact, only becoming displaced relative to one another so long as half or more of the Na^+ are retained, i.e., $x \leqslant 0.5$. Recent interest in nominal $Na_{0.5}CoO_2$ has been triggered by its potential for thermoelectric cooling;[7] a large thermoelectric power and low in-plane resistivity[8] have been reported to be accompanied by a thermal conductivity as low as that of an amorphous compound.[9] However, the thermal conductivity was measured on a polycrystalline sample of unknown water content; the hygroscopic character of the partially occupied Na layers has recently been highlighted by the report of possible superconductivity in highly hydrated nominal $Na_{0.35}CoO_2 \cdot nH_2O$.[10] In this paper, we discuss the chemistry of $Na_{1-x}CoO_2 \cdot nH_2O$ and report that the thermal conductivity of a cold-pressed, anhydrous sample of $Na_{0.57}CoO_2$ shows a conventional phonon component. In addition, we report the evolution of the lattice parameters with temperature and pressure. We interpret the anisotropic transport properties in the framework of a two-band model, a change from three-dimensional (3D) to two-dimensional (2D) itinerant-electron conduction with increasing temperature in the range $150\ \text{K} < T < 200$ K, and an in-plane bandwidth that approaches the Mott-Hubbard strong-correlation limit from the itinerant-electron side.

II. SAMPLE CHEMISTRY

Both single-crystal and polycrystalline ceramic samples were used in this study. The ceramic samples were prepared by the method described by Cushing and Wiley.[11] Stoichiometric amounts of Co metal and anhydrous NaOH were ground under an Ar atmosphere and fired at 700 °C under flowing oxygen for a total of 5 days with intermediate grindings. This method eliminates the Co_3O_4 impurities present after conventional solid-state reaction of Co_3O_4 and Na_2CO_3. Atomic absorption analysis (AAA) confirmed that the Na content in $Na_{1-x}CoO_2$ was always closer to 0.6 than to the nominal 0.5. This result is independent of the method of fabrication; it was also observed for a material synthesized from Co_3O_4 and Na_2CO_3 in air at 900 °C. To reduce the Na content further, chemical or electrochemical extraction is needed. This observation must be applicable to other samples reported in the literature that were prepared by direct reaction of precursors with Na in excess of stoichiometric proportions, samples that were assumed to be $Na_{0.5}CoO_2$. Moreover, electrochemical or chemical (with I_2 or Br_2) extraction of Na beyond $x \approx 0.5$ was found to be accompanied by a removal of oxygen as has been reported[5] for Li_xCoO_2; this situation probably applies also to $K_{1-x}CoO_2$. In addition, the material is moisture sensitive with water becoming inserted into the Na layers and expanding the *c* axis once the Na^+ content is reduced to ≈ 0.7. For this reason, we manipulated the specimen with minimum air exposure. In order to get high-density polycrystalline samples, the anhydrous powders were cold pressed under 80–100 kbar and then annealed at 900 °C.

Single crystals ($1.5 \times 1.5 \times 0.01\ \text{mm}^3$) were grown from a NaCl flux. Co_3O_4, Na_2CO_3, and NaCl were mixed in a molar ratio Na:Co:NaCl=1:1:7, placed in an alumina boat, and fired at 950 °C for 12 h. The temperature was then slowly reduced to 850 °C at 0.5 °C/h, and then fired at 180 °C/h to room temperature.

A four-probe method was used to measure the resistivity. Magnetization was measured with a superconducting quantum-interference device magnetometer (Quantum Design). Thermal conductivity was measured with a steady-

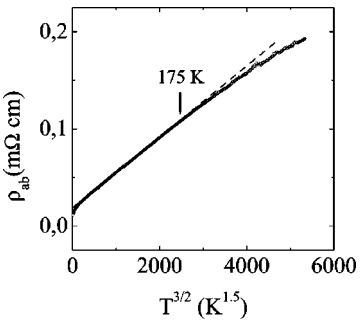

FIG. 1. Temperature dependence of the resistivity along the *ab* plane versus $T^{3/2}$.

state method; the temperature gradient was controlled to be less than 1% of the base temperature. The powder x-ray diffraction under pressure was performed in a diamond-anvil cell mounted on a four-circle goniometer. The x-ray beam (2.0 kW) was generated from a Mo target in a sealed tube and monochromated by a graphite crystal. NaCl or Au powder mixed with the sample powder and epoxy (no hardener component) was used as the pressure manometer. Powder-diffraction peaks show no broadening in pressures up to 5 GPa; they were collected by a Fuji image plate and integrated into a one-dimensional $I \sim 2\theta$ curve with the program FIT2D.

III. RESULTS AND DISCUSSION

Figure 1 shows the in-plane resistivity $\rho_{ab}(T^{3/2})$ for $Na_{0.57}CoO_2$. In view of a transition from polaronic to itinerant in-plane conduction as x increases beyond $x \approx 0.25$ in $Na_{1-x}CoO_2$, [12] we have attributed the $T^{3/2}$ behavior of $\rho_{ab}(T)$ below 175 K, where the compound exhibits 3D metallic behavior, to the presence of strong-correlation fluctuations persisting into the compositions with $x > 0.25$. This departure from conventional Fermi-liquid behavior was rationalized within the context of a 3D electron gas,[13] a condition that breaks down progressively above 170 K where the *c*-axis conductivity becomes thermally activated.[7,14] Figure 2 shows the pressure dependence of the thermoelectric power α(T) of $Na_{0.57}CoO_2$. The large temperature dependent α(T) has a slope change near $\approx$100 K that progressively decreases as the pressure increases.

Figure 3 shows the evolution of the room-temperature lattice parameters with pressure $P < 45$ kbar for the powder crushed from single crystals. Although the structure undergoes no symmetry change in this pressure range, a first-order transition at $P \approx 35$ kbar separates the low-pressure phase with a large compressibility from the high-pressure phase, which is less compressible.

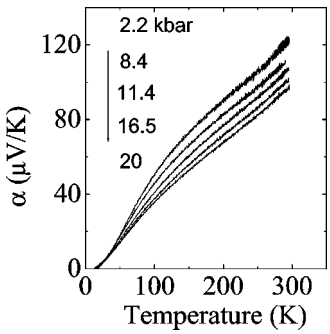

FIG. 2. Thermoelectric power under pressure of a dense (cold-pressed) polycrystalline sample.

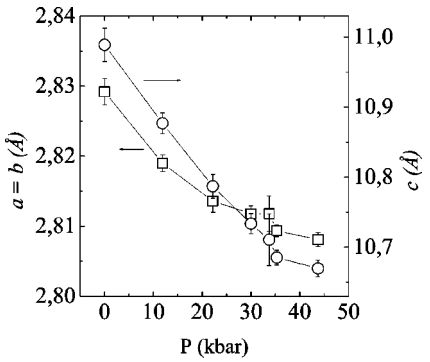

FIG. 3. Pressure dependence of the room-temperature lattice parameters obtained in a powder from crushed single crystals. Lines are guides to the eye.

The thermal-expansion data of Fig. 4 were taken from a polycrystalline sample having the same lattice parameters as that of a single crystal at room temperature. However, the moisture sensitivity of the polycrystalline sample complicated the measurement of the thermal expansion, giving relatively broad x-ray-diffraction peaks and introducing some error in the values of $a = b$ and c. Nevertheless, Fig. 4 shows clearly that the in-plane thermal expansion below room temperature is negligible whereas the *c*-axis thermal expansion is relatively large.

This quite unusual variation of lattice parameters with temperature and pressure complements the transport data and can be understood from the virial theorem of classic mechanics, which states that for central-force fields

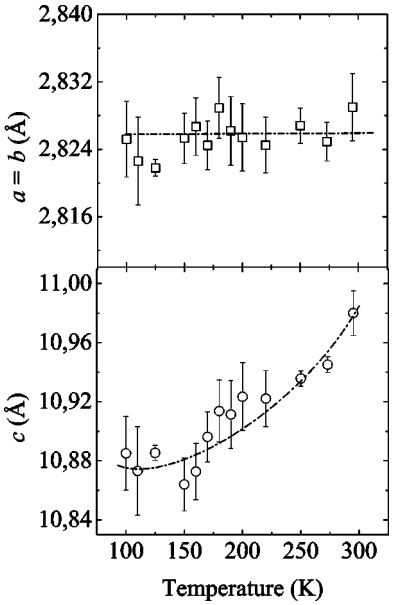

FIG. 4. Thermal evolution of the in-plane (above) and along the *c*-axis (below) lattice parameters of a polycrystalline sample. Si was used as an internal standard. Lines are guides to the eye.

$$2\langle \mathrm{T}\rangle + \langle \mathrm{V}\rangle = 0, \tag{1}$$

where the mean kinetic energy $\langle \mathrm{T}\rangle$ of a system of electrons decreases discontinuously if the mean volume of the electrons increases discontinuously across a localized to itinerant electronic transition. Since the electrons are bound, their mean potential energy $\langle \mathrm{V}\rangle$ is negative, and a discontinuous decrease in $\langle \mathrm{V}\rangle$ for antibonding electrons is accomplished by a discontinuous decrease in the equilibrium M-O bond length. Therefore, crossover occurs at a first-order transition with the localized-electron equilibrium bond length larger than the equilibrium itinerant-electron bond length, i.e., $(M\text{-O})_{\mathrm{loc}} > (M\text{-O})_{\mathrm{itin}}$. It follows that where the two phases coexist, the double-well potential for the equilibrium M-O bond length gives an average $\langle M\text{-O}\rangle$ that is highly compressible and that pressure stabilizes the itinerant-electron phase relative to the localized-electron phase.[15] In order to apply this reasoning to the $Na_{1-x}CoO_2$ system, we first recognize that the threefold-degenerate t_2 orbitals at the low-spin, octahedral-site cobalt atoms are split by the hexagonal symmetry into an a_1^T orbital directed along the c axis and twofold-degenerate e^T orbitals directed toward neighboring cobalt atoms of a CoO_2 plane.[16] The observation[12] of a transition from polaronic to itinerant electrons in the CoO_2 planes as x increases to beyond $x=0.28$ shows that in $Na_{0.57}CoO_2$, the Co-Co interactions in the CoO_2 planes are strong enough to broaden the e^T orbitals into a narrow band of mostly itinerant-electron states, but the large compressibility within these planes in the pressure range $0<P<35$ kbar is understandable from the virial theorem if strong-correlation fluctuations persist in this band, as was deduced previously[13] to account for the $T^{3/2}$ dependence of $\rho(T)$ below 175 K. The observation[7] of a smooth transition from a metallic to a polaronic temperature dependence of the c-axis conductivity in the interval $150\ \mathrm{K}<T<250\ \mathrm{K}$ is characteristic of a transition from itinerant $a_1{}^T$ electrons at lowest temperatures to polaronic $a_1{}^T$ electrons at room temperature, the two phases coexisting in the crossover temperature interval $150\ \mathrm{K}<T<250\ \mathrm{K}$. Since pressure increases the c-axis Co-O-O-Co interactions, it follows from the virial theorem that we should expect a large c-axis compressibility at room temperature where there is a smooth, two-phase transition back to itinerant $a_1{}^T$ electrons. We therefore identify the large c-axis compressibility up to 35 kbar with a two-phase transition at room temperature from polaronic back to itinerant behavior of $a_1{}^T$ electrons. The existence of a narrow $a_1{}^T$ band of itinerant-electron states requires unusually strong Co-O-O-Co interactions along the c axis. How this is possible is made evident by the observation of O_2 evolution from the CoO_2 sheets on the extraction of more than half of the Na atoms. The evolution of oxygen occurs on oxidation of a redox couple that is pinned at the top of an $O^{2-}{:}2p^6$ band.[17] Pinning of a redox couple occurs where the redox couple lies below the $O^{2-}{:}2p^6$ energy level in a point-charge model; covalent mixing of M-$3d$ and O-$2p$ states lifts the antibonding states to the top of the $O{:}2p^6$ bands. These antibonding states have the symmetry of the $3d$ orbitals, but a dramatic increase in the O-$2p$ component of these states occurs where the cationic redox couple falls below the $O^{2-}{:}2p^6$ energy in the point-charge model. In $Na_{1-x}CoO_2$, the low-spin Co(IV)/Co(III) redox couple falls below the O-$2p_\pi$ states of the point-charge $O^{2-}{:}2p^6$ energies, and the predominantly O-$2p_\pi$ character of the holes introduced into the pinned antibonding band allows them to combine in surface states to form O_2^{2-} peroxide ions followed by O_2 evolution. It is the strong O-$2p_\pi$ character of the ligand-field t_2 orbitals of the formal Co(IV)/Co(III) redox couple pinned at the top of the $O^{2-}{:}2p^6$ band that is responsible for the sizable Co-O-O-Co overlap integral of the $a_1{}^T$ orbitals.

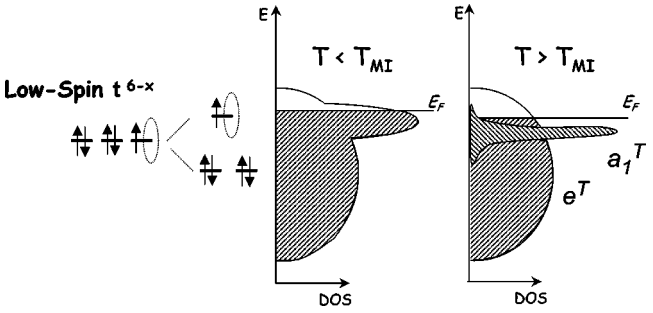

FIG. 5. Schematic band diagram of the system Na_xCoO_2. The dotted circle represents a hole introduced by Co^{4+}. T_{MI} is the temperature at which the resistivity becomes thermally activated along the c axis (see Refs. 7 and 14).

Figure 5 is a schematic representation of the antibonding e^T and $a_1{}^T$ bands pinned at the top of the nominal $O^{2-}{:}2p^6$ bands. Narrowing of the a_1^T band on raising the temperature in the interval $0<T<300$ K reflects the transition from itinerant to polaronic (or variable-range hopping) behavior of the $a_1{}^T$ electrons. Placement of the $a_1{}^T$ band relative to the Fermi energy E_F is deduced from considerations of the thermoelectric power and the thermal-expansion data, and it is consistent with elaborated band-structure calculations.[18]

From the virial theorem, the large thermal expansion of the c axis reflects the change in the $(M\text{-O})_{\mathrm{loc}}/(M\text{-O})_{\mathrm{itin}}$ ratio as the volume fraction of the polaronic phase among the a_1^T electrons increases with temperature. On the other hand, the e^T orbitals are broadened into a band of itinerant-electron states by Co-Co interactions. The strength of these interactions is also enhanced by the covalent admixture of O-$2p$ character into the Co-$3d$ orbitals. However, the e^T bands are also at the narrow-band limit for itinerant-electron behavior, and a thermal expansion of the Co-Co separation would induce polaronic behavior, which would increase the basal-plane thermal expansion in a positive feedback. Since this situation is not observed, it is apparent that $Na_{0.57}CoO_2$ adjusts its c axis so as to retain a nearly constant Co-Co distance in the plane with increasing temperature. By expanding the c axis, which induces a transformation to polaronic behavior of the $a_1{}^T$ holes, electrons can be transferred from the e^T bands to the $a_1{}^T$ bands so as to retain the Co-Co separation. This interpretation is supported by the almost identical in-plane Co-Co distances in $A_{1-x}CoO_{2-\delta}$, $Co^{3+}/Co^{4+}\approx 1$, when A goes from Li to Na to K and even Sr, in spite of the large variation of the Co-Co distance along the c axis. Therefore, we place the Fermi energy in both the $a_1{}^T$ and e^T bands, and E_F near the top of the $a_1{}^T$ band is needed in

order to account for the thermoelectric power. The general expression for the thermoelectric power as derived from the Boltzmann equation is[19]

$$\alpha = \frac{1}{e\sigma T}\int (E-E_F)\sigma(E)\frac{\partial f}{\partial E}dE, \tag{2}$$

where f is the Fermi-Dirac distribution function and $\sigma(E)$ is defined in the expression of the dc conductivity, σ,

$$\sigma = \int \sigma(E)\frac{\partial f}{\partial E}dE. \tag{3}$$

For a normal broadband metal, Mott and Jones[20] assumed that $\sigma(E) \propto E^x$ in the neighborhood of E_F to obtain the expression

$$\alpha \approx \frac{\pi^2 k_B^2 T}{3eE_F}x. \tag{4}$$

In our narrow-band case, E_F, as measured from the top of the bands, is small and x depends on the curvature of E_k vs k. Although the Mott Eq. (4) may not be applicable to the crossover from itinerant to polaronic behavior, nevertheless the extreme asymmetry of the density of states on either side of E_F as pictured in Fig. 5 can be expected to account, according to Eq. (2), for the large value of $\alpha(T)$. The thermoelectric power is sensing the energy dependence of the density of states around E_F. From the general expression of Eq. (2) it can be deduced that when $N(E)$ is an even function around E_F, α goes to zero, but increases as the asymmetry in $N(E)$ in the interval $E_F \pm k_B T$ does. From the band diagram of Fig. 5, $N(E)$ changes rapidly with energy near $E=E_F$ which produces a considerable enhancement of α as the $a_1{}^T$ band narrows with temperature. A reduction in the hole doping (increasing the Na content per formula unit close to 0.75) places the E_F further above the $a_1{}^T$ band, which makes the thermopower smaller (as is observed) in spite of the lower conductivity of the $x=0.7$ compound.

Moreover, $\alpha(T)$ also appears to reflect the electron transfer that was postulated to suppress the thermal expansion of the Co-Co bond in the CoO_2 planes. Reduction of the holes in the $a_1{}^T$ band increases the contribution to $\alpha(T)$ from the $a_1{}^T$ holes more strongly than it decreases the contribution to $\alpha(T)$ from the e^T holes, so $\alpha(T)$ is enhanced where the $a_1{}^T$ band is narrowed by the c-axis thermal expansion. Suppression by pressure of the narrowing of the $a_1{}^T$ band reduces the electron transfer from the e^T to the $a_1{}^T$ bands and hence the change in slope of $\alpha(T)$ near 100 K.

Recently, Wang *et al.*[21] reported a strong suppression of the ab-plane thermopower in a longitudinal magnetic field. From these results the spin entropy was suggested to dominate the enhanced thermopower in this material. Since the spin entropy should not be influenced by pressure, a 20% reduction at room temperature under 20 kbar that we report here could not be interpreted without taking into account the important effect of the asymmetry in $N(E)$ close to E_F.

The coexistence of localized spins and itinerant electrons adds a Curie-Weiss term to the Pauli paramagnetism to give a temperature dependence to the paramagnetic susceptibility

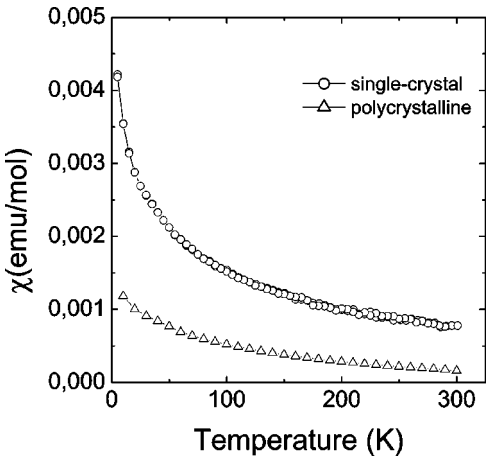

FIG. 6. Temperature dependence of the magnetic susceptibility along the ab plane of a single crystal (circles) and in a polycrystalline sample (triangles).

of $Na_{0.57}CoO_2$ (Fig. 6). This temperature dependence is present in the susceptibility of polycrystalline materials and for the ab plane of single crystals. The coexistence of strong-correlation fluctuations and itinerant-electron behavior can be expected to introduce bond-length fluctuations that suppress the phonon contribution to the thermal conductivity, as has been observed in the $RNiO_3$ family of perovskites.[22] In fact, a suppressed thermal conductivity characteristic of an amorphous compound has been reported[9] for nominal $Na_{0.5}CoO_2$. In order to check this result, the thermal conductivity $\kappa(T)$ was measured on a sample prepared from a cold-pressed polycrystalline powder that was resintered at 900 °C to grow its grain size. After this treatment, the AAA showed no significant change in the Na/Co ratio. Figure 7 shows the ambient-pressure $\kappa(T)$ curve. It is evident that a sizable phonon and/or spin component is observed with no apparent suppression in the interval $150\ \text{K} < T < 250\ \text{K}$ where the transition from itinerant to polaronic $a_1{}^T$ electrons has been deduced. This result will certainly reduce the thermoelectric figure of merit of the material, and hence the expectations about its possible technological applicability.

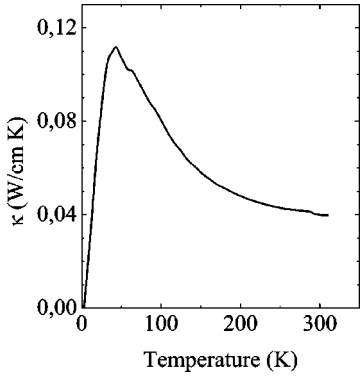

FIG. 7. Temperature dependence of the lattice thermal conductivity of a cold-press sintered polycrystalline sample. The electronic contribution was subtracted using the Wiedeman-Franz law and the experimental resistivity of the sample.

Since the random distribution of Na^+ ions in the Na planes perturbs the c-axis periodic potential, we introduce Anderson-localized states at the wings of the narrow $a_1{}^T$ band; the polaronic $a_1{}^T$ holes may, in fact, be trapped in these states. In this case, the polaronic phase does not fluctuate, and any suppression of the phonon contribution to $\kappa(T)$ in $Na_{0.57}CoO_2$ would come from strong-correlation fluctuations in the e^T bands. But in this compound, either the volume fraction of strong-correlation fluctuations in the e^T bands is too small to suppress the phonons completely or κ is enhanced by spin excitations.[23] Comparison of $\kappa(T)$ for the $RNiO_3$ family shows that retention of a significant phonon contribution to $\kappa(T)$ is consistent with a minor volume fraction of strong-correlation fluctuations among the e^T electrons.

IV. CONCLUSIONS

From this study, we can draw the following conclusions:

(i) The nominal compositions $Na_{0.5}CoO_2$ reported in the literature are probably closer to $Na_{0.6}CoO_2$ unless additional Na was extracted chemically or electrochemically. Moreover, these compositions are moisture sensitive, so measured samples may contain an unknown amount of water unless specific precautions are taken to avoid prolonged exposure to humid air.

(ii) Oxygen evolution on extraction of more than half the sodium from $NaCoO_2$ signals that the nominal Co(IV)/Co(III) redox couple is pinned at the top of the nominal O^{2-}:$2p^6$ bands, which introduces a dominant O-$2p_\pi$ character into the antibonding $a_1{}^T$ and e^T bands of the low-spin cobalt atoms. Consequently, the Co-O-O-Co c-axis interactions and the Co-Co basal-plane interactions are just strong enough to make itinerant at lowest temperatures the $a_1{}^T$ and e^T holes introduced into these bands by the removal of $\approx$0.43 sodium atoms in $Na_{0.57}CoO_2$.

(iii) A large c-axis thermal expansion in the temperature interval $150\ \mathrm{K} < T < 250\ \mathrm{K}$ correlates with a smooth transition from a metallic to a nonmetallic temperature dependence of the c-axis resistivity $\rho(T)$; the basal-plane resistivity remains metallic for all temperatures $T < 300$ K, varying as $T^{3/2}$ below $T = 175$ K, and the Co-Co separation holds essentially constant throughout the range $77\ \mathrm{K} < T < 300\ \mathrm{K}$. From the virial theorem, the smooth transition in $\rho(T)$ may be interpreted to reflect a first-order transition with the coexistence of two electronic phases for localized (polaronic) and itinerant $a_1{}^T$ holes with $(\text{Co-O})_{\text{loc}} > (\text{Co-O})_{\text{itin}}$. Electron transfer from the e^T band to the overlaping $a_1{}^T$ band with increasing temperature can account for a temperature-independent Co-Co separation below 300 K.

(iv) A first-order transition from a phase with polaronic holes to one with itinerant holes in the e^T bands is found as x increases in $Na_{1-x}CoO_2$, and a large basal-plane room-temperature compressibility in the pressure range $P < 35$ kbar as well as the $\rho_{ab} \propto T^{3/2}$ dependence below 175 K are consistent with retention of a minority volume of strong-correlation fluctuations in the e^T bands at $Na_{0.57}CoO_2$. An anomalously large room-temperature c-axis compressibility of $Na_{0.57}CoO_2$ up to 35 kbar may be logically assumed to reflect a smooth transition back to metallic holes in the a_1^T band at room temperature in this pressure range.

(v) The large thermoelectric power $\alpha(T)$ and its pressure dependence may be interpreted with this model if the top of the narrow $a_1{}^T$ band is located near E_F so as to give a large curvature of the E_k vs k curves near E_F.

(vi) The phonon or magnon component of the thermal conductivity is not suppressed in a cold-pressed, anhydrous ceramic sample which shows nearly intrinsic properties. Applicability of this material for thermoelectric cooling could be not as direct as previously thought.

ACKNOWLEDGMENTS

We want to acknowledge Dr. Brian Chushing and Dr. Elin Winkler for helpful discussions and comments during the preparation and analysis of the materials. The authors thank the NSF, the Robert A. Welch Foundation, Houston, Texas, and the TCSUH of Houston, Texas for financial support. F.R. would like to thank the Fulbright Foundation and MECD (Spain) for financial support.

[1] C. Delmas, C. Fouassier, and P. Hagenmuller, Physica B & C **99**, 81 (1980).

[2] K. Mizushima, P. C. Jones, P. I. Wiseman, and J. B. Goodenough, Mater. Res. Bull. **15**, 783 (1980).

[3] M. Menetrier, I. Saadonne, S. Levasseur, and C. Delmas, J. Mater. Chem. **9**, 1335 (1999).

[4] J. B. Goodenough, *Proceedings of the Electrochemical Society 99-24*, edited by G.-A. Nazri *et al.* (Electrochemical Society, Pennington, NJ, 2000), p. 1.

[5] S. Venkatraman and A. Manthiram, Chem. Mater. **14**, 3907 (2002).

[6] J. B. Goodenough, K. Mizushima, and T. Takeda, Jpn. J. Appl. Phys. **19**, 305 (1980).

[7] I. Terasaki, *Proceedings of the 18th International Conference on Thermoelectrics (ICT '99)* (IEEE, Piscataway, NJ, 2000), p. 569.

[8] I. Terasaki, Y. Sasago, and K. Uchirokura, Phys. Rev. B **56**, R12685 (1997).

[9] K. Takahata, Y. Iguchi, D. Tanaka, T. Itoh, and I. Terasaki, Phys. Rev. B **61**, 12551 (2000).

[10] K. Takada, H. Sakurai, E. Takayama-Muromachi, F. Izumi, R. A. Dilanian, and T. Sasaki, Nature (London) **422**, 53 (2003).

[11] B. L. Cushing and J. B. Wiley, J. Solid State Chem. **141**, 385 (1998).

[12] J. Molenda, Solid State Ionics **21**, 263 (1986).

[13] F. Rivadulla, J.-S. Zhou, and J. B. Goodenough, Phys. Rev. B **67**, 165110 (2003).

[14] T. Valla, P. D. Jonson, Z. Yusof, B. Wells, Q. Li, S. M. Loureiro, R. J. Cava, M. Mikami, Y. Mori, M. Yoshimura, and T. Sasaki, Nature (London) **417**, 627 (2002).

[15] J. B. Goodenough, in *Physics of Manganites*, Fundamental Mate-

rials Research Series, edited by T. A. Kaplan and S. P. Mahanti (Kluwer Academic/Plenum, New York, 1999), p. 127.
[16] J. B. Goodenough, in *Magnetism and the Chemical Bond* (Wiley, New York, 1963).
[17] J. B. Goodenough, in *Advances in Lithium-Ion Batteries*, edited by W. A. Schalkwijk and B. Scrosati (Kluwer Academic/Plenum, New York, 2002), p. 135.
[18] D. J. Singh, Phys. Rev. B **61**, 13397 (2000).
[19] D. K. C. MacDonald, *Thermoelectricity: An Introduction to the Principles* (Wiley, New York, 1962).
[20] N. F. Mott and H. Jones, in *The Theory of the Properties of Metals and Alloys* (Clarendon, Oxford, 1936).
[21] Y. Wang, N. S. Rogado, R. J. Cava, and N. P. Ong, Nature (London) **423**, 425 (2003).
[22] J.-S. Zhou, J. B. Goodenough, and B. Dabrowski, Phys. Rev. B **67**, 020404(R) (2003).
[23] C. Hess, C. Baumann, U. Ammerahl, B. Büchner, F. Heidrich-Meisner, W. Brening, and A. Revcolevschi, Phys. Rev. B **64**, 184305 (2001).